Electronic Supplementary Information

Advanced Morphological Control over Cu Nanowires through a Design of Experiments Approach

Andrea Conte,[a] Antonella Rosati,[a] Marco Fantin,[a] Alessandro Aliprandi,[a] Marco Baron,[a] Sara Bonacchi,[a] and Sabrina Antonello[a,*]

Department of Chemical Sciences, University of Padova, Via F. Marzolo 1, 35131, Padova, Italy

Contents List

1. Additional figures

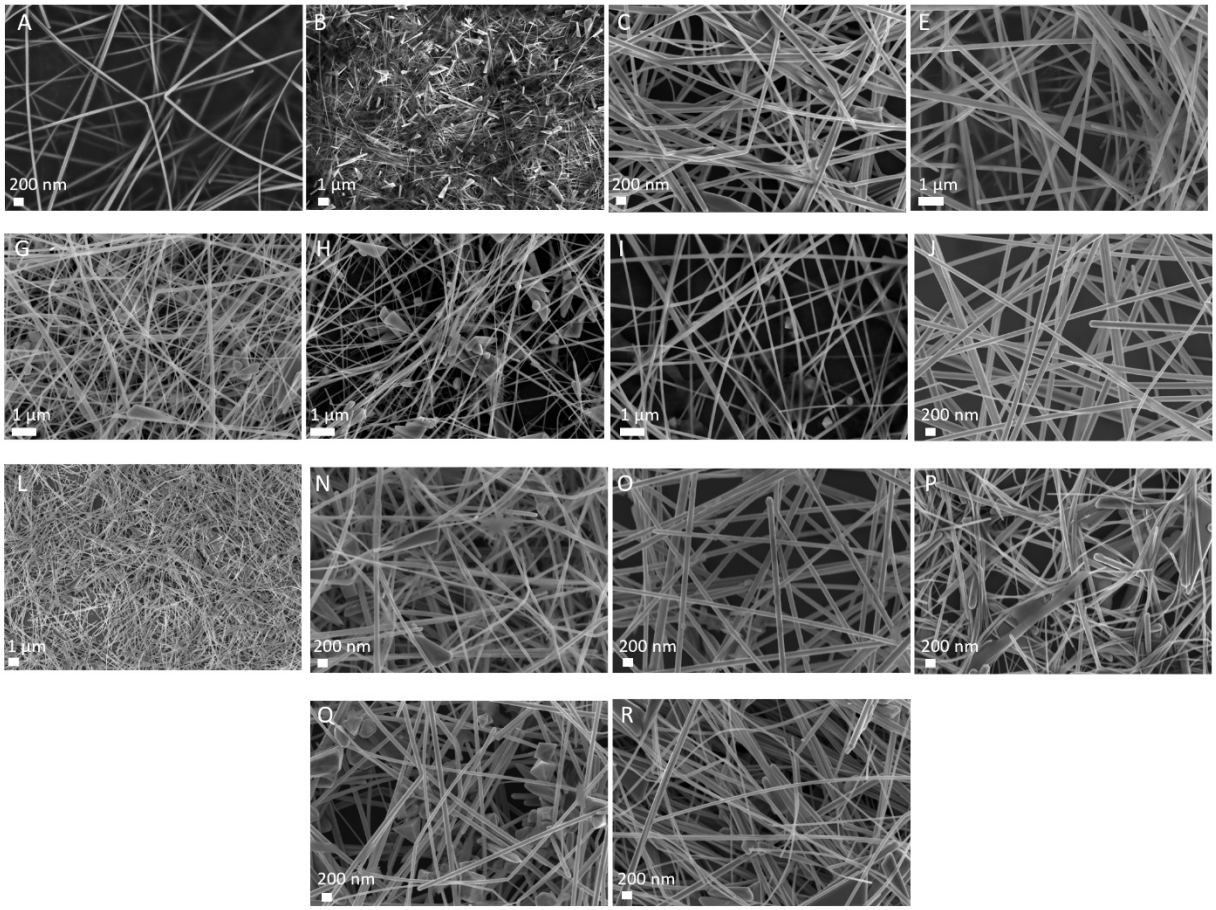

Fig. S1. SEM of CuNWs obtained from glucose synthesis route: A, B, C, E, G, H, I, J, L, N, O, P, Q, R.

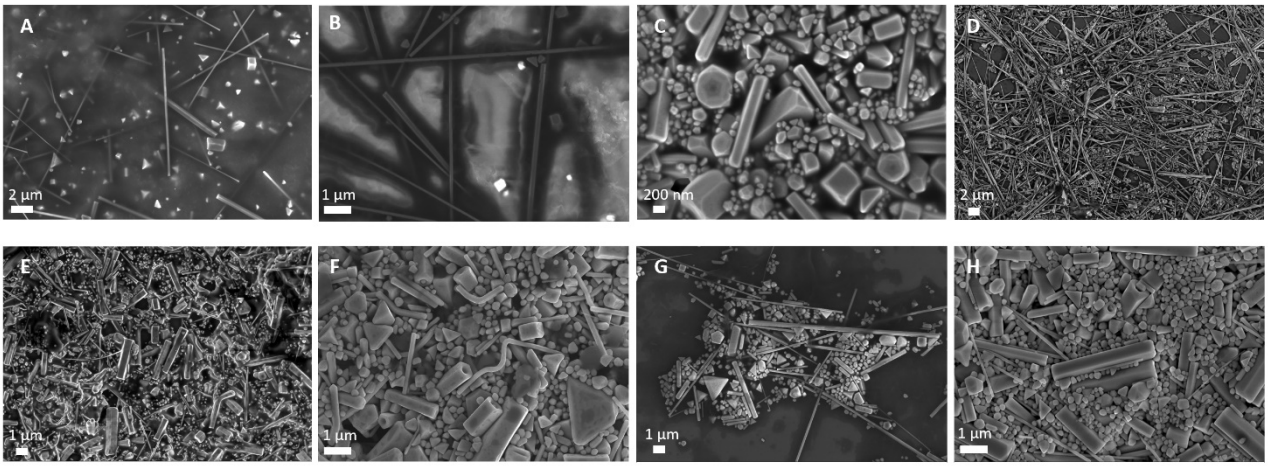

Fig. S2. SEM images of ascorbate synthesis route: A, B, C, D, E, F, G, H.

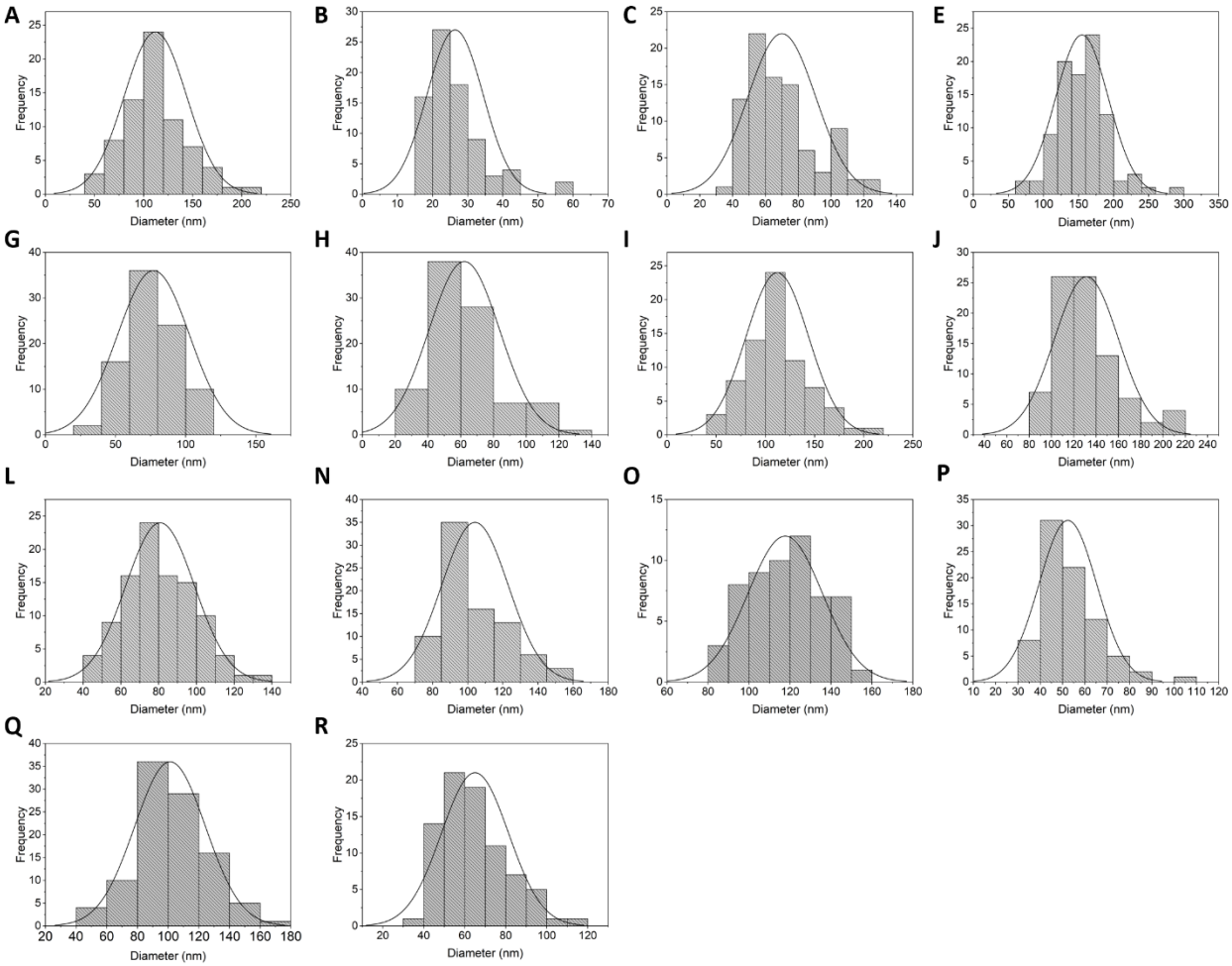

Fig. S3. Histograms of diameter distribution of CuNWs synthesized via glucose route.

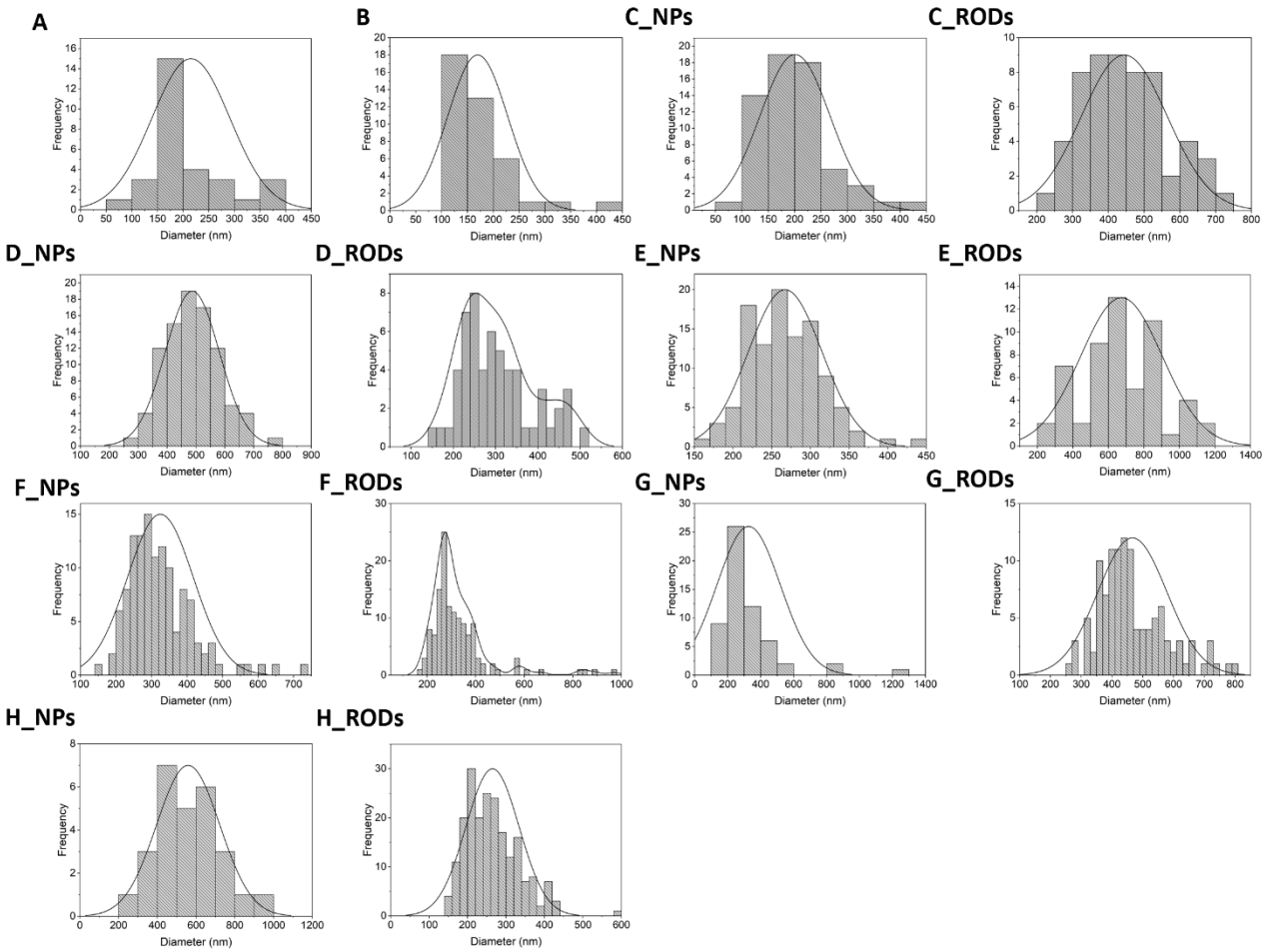

Fig. S4 Histograms of diameter distribution of nanoparticles (NPs) and nanorods (NRODs) synthesized via ascorbate route.

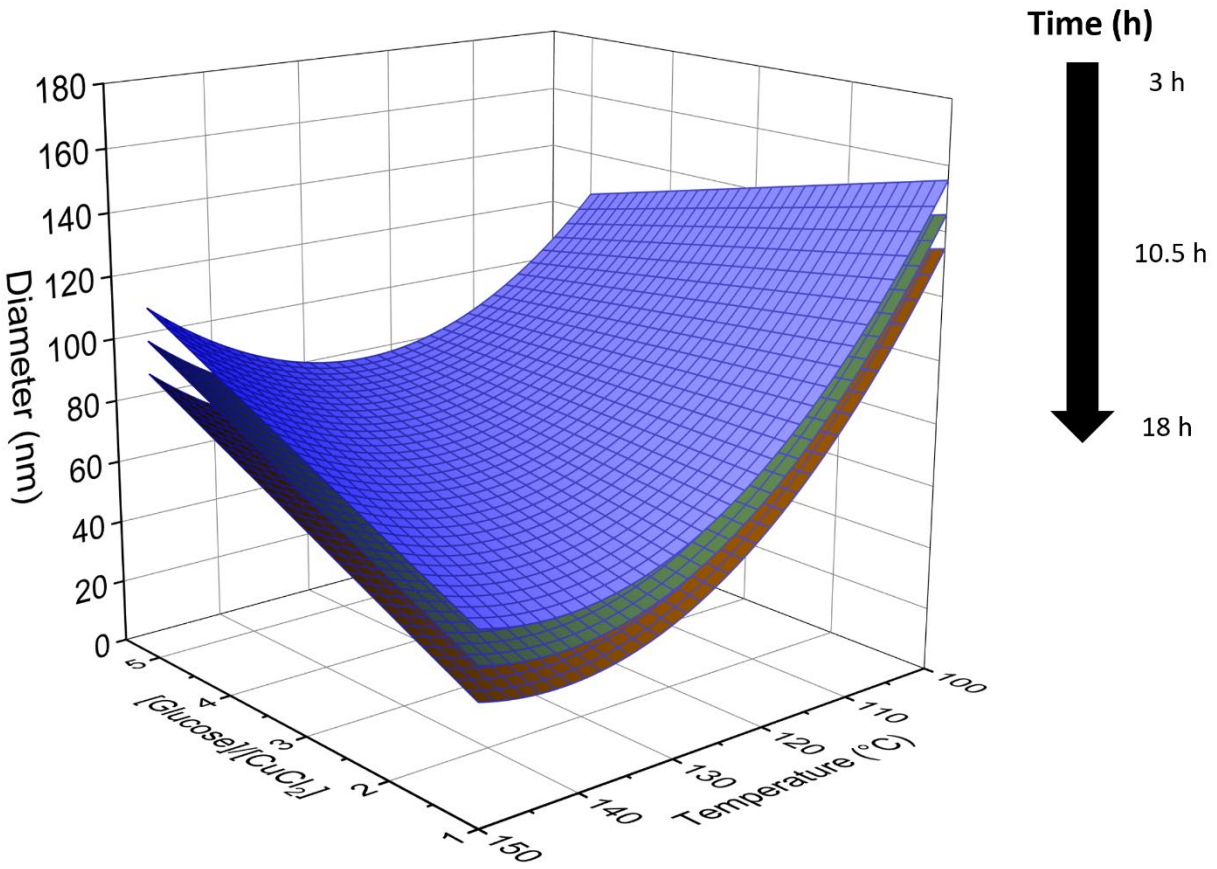

Fig. S5. 3D map of CuNWs diameter at different fixed time, calculated by Eq. 1 by fixing the time at 3, 10.5, and 18 h respectively. The black arrow shows the variation in offset of the surface which describes the diameter of CuNWs by increasing the reaction time. The surfaces correspond to 3 h (blue), 10.5 h (green), and 18 h (orange) respectively.

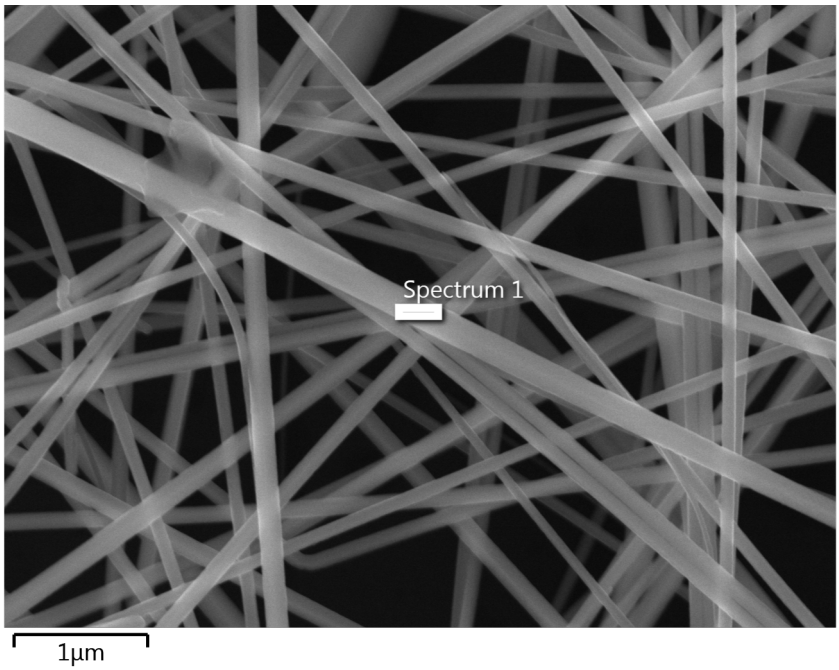

Fig. S6. SEM image of J^{glu} synthesis. The white spot concerns the region of EDX investigation.

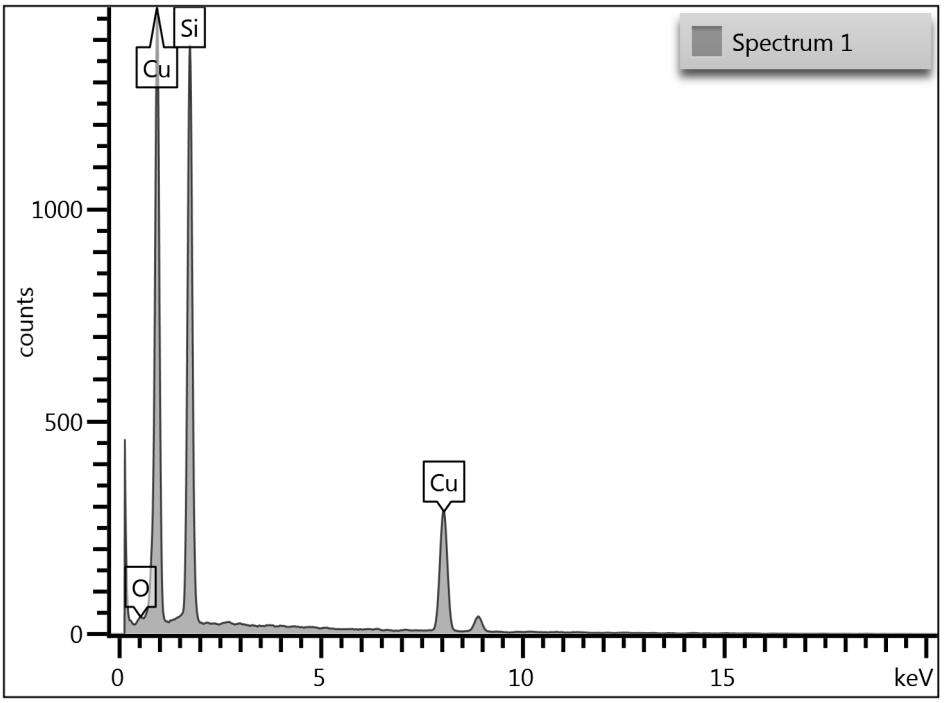

Fig. S7. EDX spectrum of J^{glu} synthesis. Silicon signal is due to the sample holder.

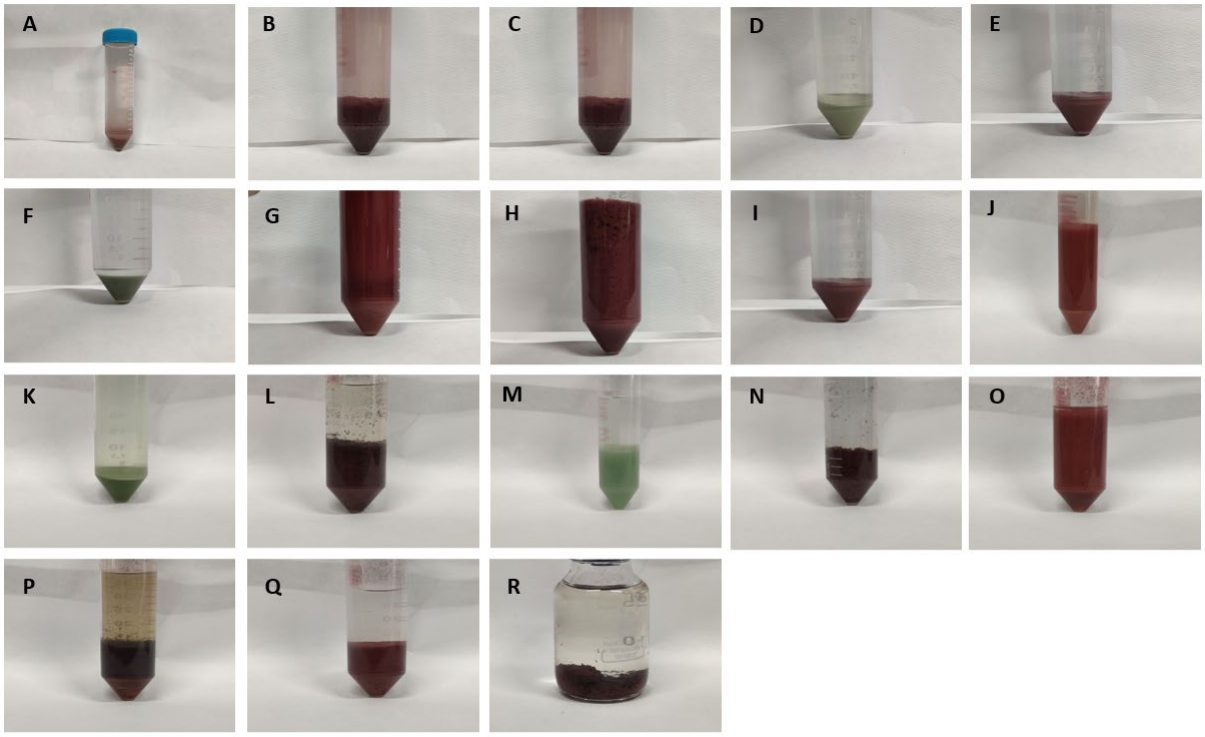

Fig. S8. Photos of synthesis products produced through the glucose route. The products were stored in absolute ethanol. The letters refer to the order reported in Table 2.

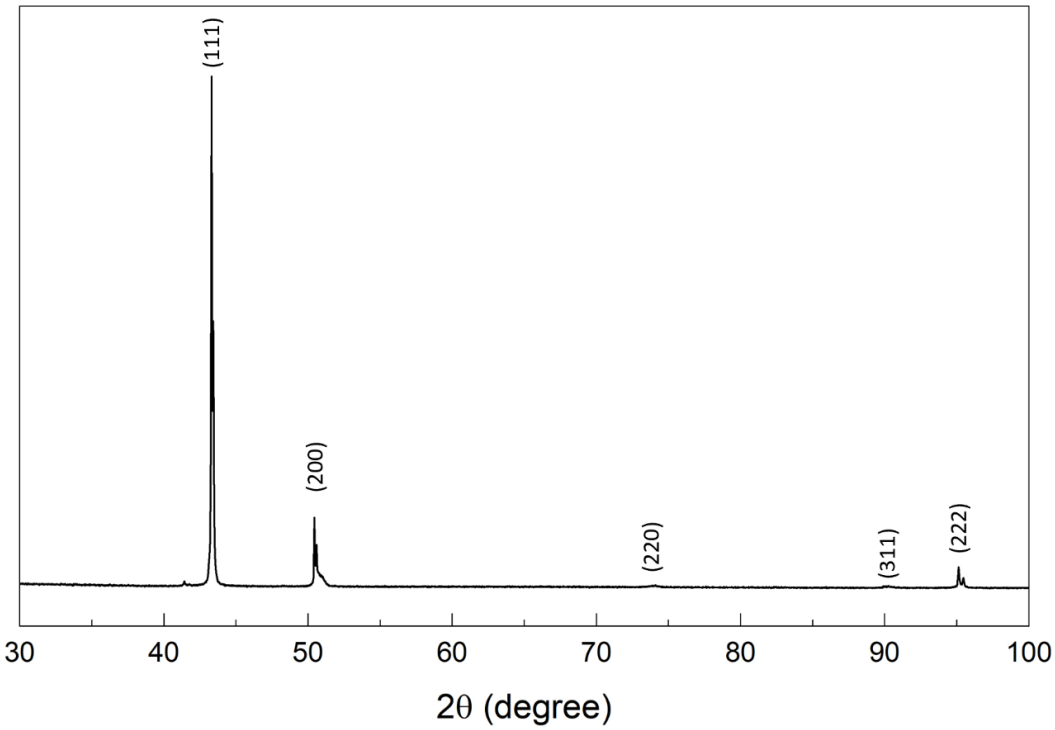

Fig. S9. XRD diffractogram of CuNWs (J^{glu}), the peaks are labeled according to the crystal facet that represented.

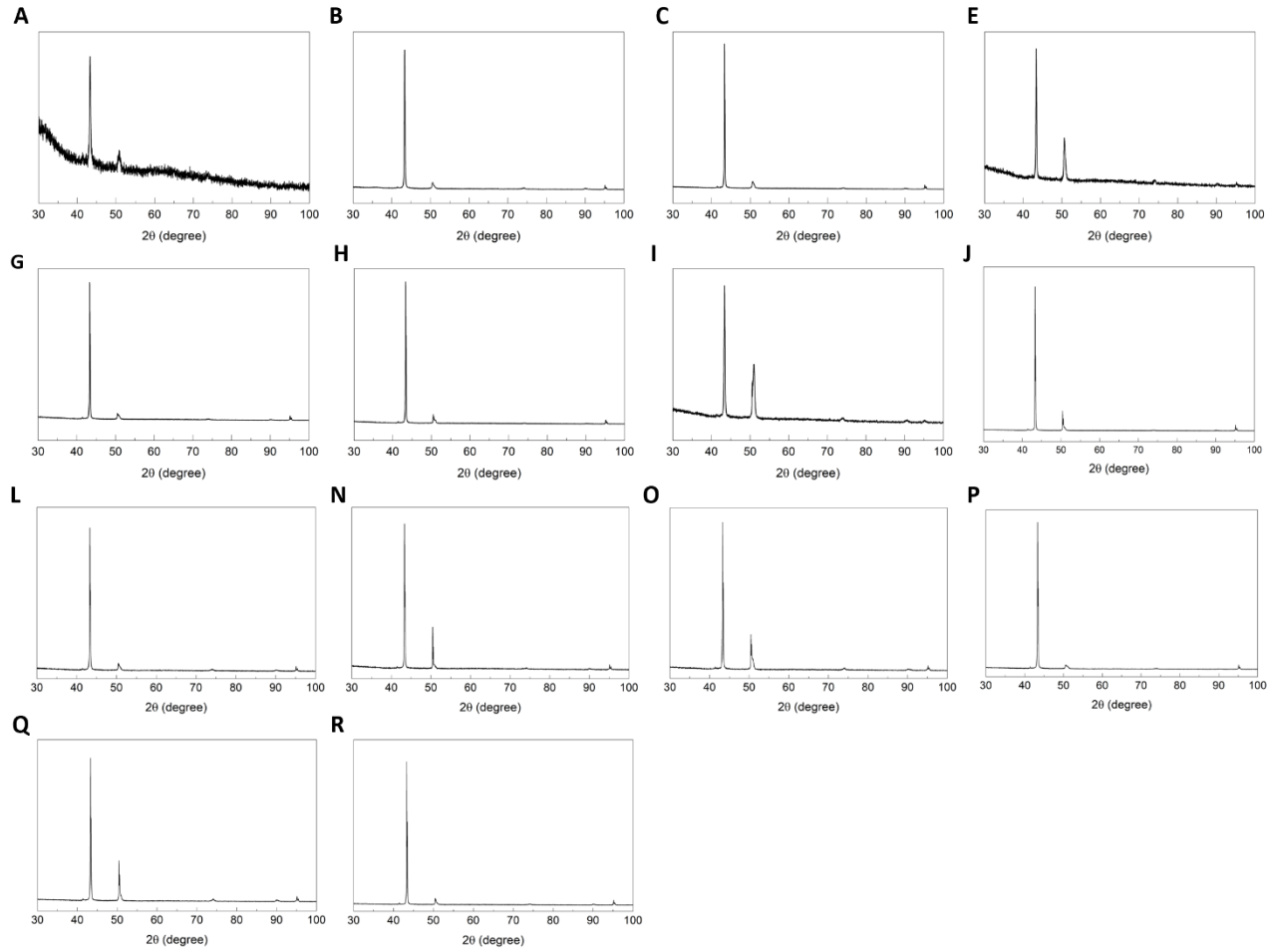

Fig. S10. XRD diffractograms of CuNWs synthesized through glucose route. The letters refer to the order reported in Table 2.

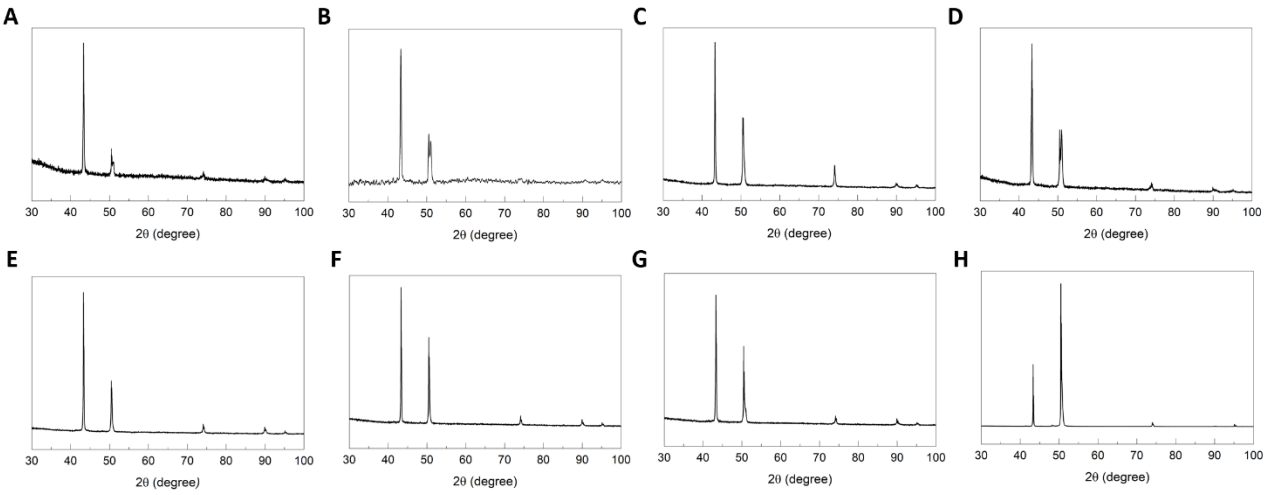

Fig. S11. XRD diffractograms of CuNWs synthesized through sodium ascorbate route. The letters refer to the order reported in Table 3.

Optimization of CuNWs properties via desirability functions

Derringer and Suich introduced the Desirability function as a solution for optimizing multiple responses in industrial settings.[2] Desirability function allowed us to find the optimal experimental conditions (factor levels) to reach, simultaneously, the optimal value for all the evaluated outputs (diameter, yield, and XRD aspect ratio). Using the software JMP, our procedure was as follows:

1. Prediction formulas for the measured output (diameter, yield, and XRD-derived aspect ratio) were obtained (see Eq. 1-3 in main text).
2. Via software, the desired output was set either to maximize (e.g. see desirability column for Yield % in Fig. S12A) or minimize (e.g. see desirability column for diameter in Fig. S13A).
3. The software calculated the optimal experimental conditions (temperature, time, and equivalents of glucose) to obtain the desired outputs set in point 2. (The optimized conditions are presented in red in Figure S13.)

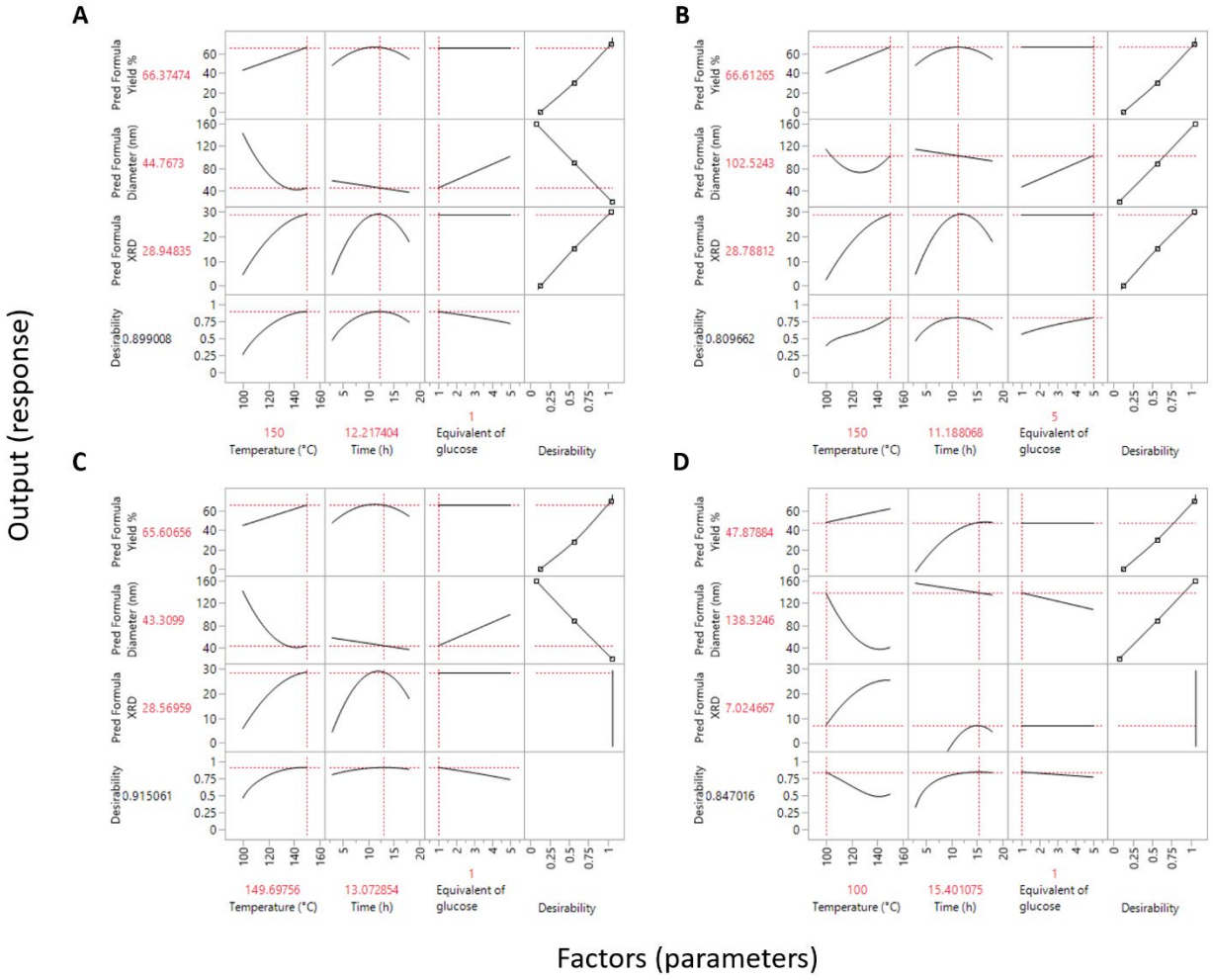

Fig. S12. Optimization of synthesis conditions to target specific physicochemical parameters of CuNWs for different potential applications.[3] A), B), C), D).

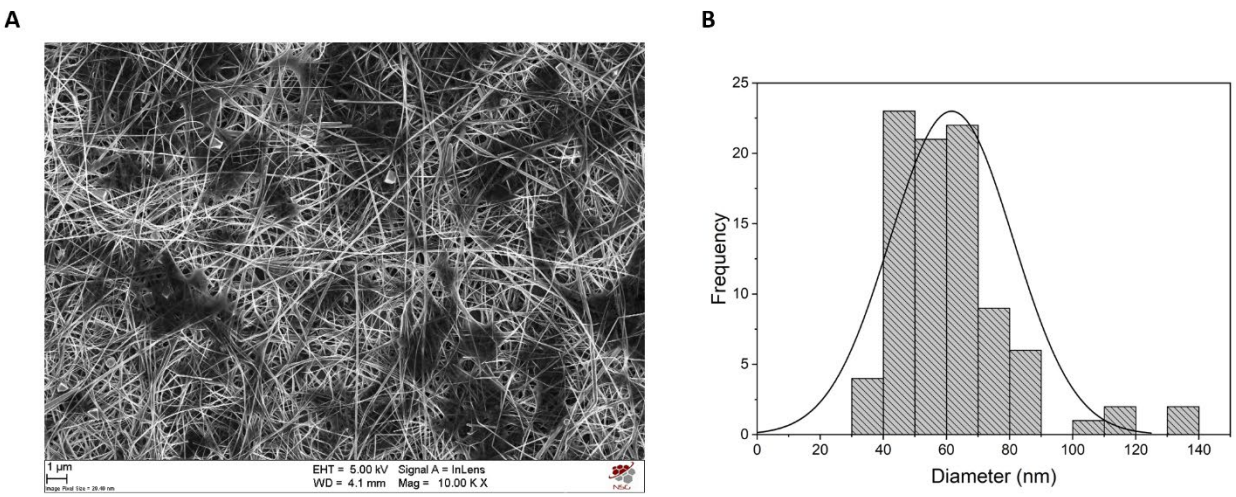

Fig. S13. A) SEM image of 0.5 equivalent, 150°C, 3h, through ascorbate synthesis route. B) Histogram of diameter distribution of CuNWs synthesized via ascorbate route, 0.5 equivalent, 150°C, 3h.

2. Additional tables and procedures

Table. S1. Relevant statistical parameters for the obtained models describing diameter, yield and Ψ, including p-value and % contribution of each factor.

	Diameter		Yield		Ψ	
Factor	***p*-Value[a]**	**% Contribution[b]**	***p*-Value[a]**	**% Contribution[b]**	***p*-Value[a]**	**% Contribution[b]**
t	0.1	11.8	$< 10^{-4}$	25.9	0.2[b]	6.1
T	0.2[b]	11.9	$< 10^{-4}$	25.9	0.002	23.5
[R]	0.06	12.6	>0.1	—	>0.1	—
t·T	>0.1	—	0.006	20.1	0.03	17.4
t·[R]	>0.1	—	>0.1	—	>0.1	—
T·[R]	0.003	24.3	>0.1	—	>0.1	—
T·T	0.01	39.5	>0.1	—	0.09	11.8
t·t	>0.1	—	0.04	28.1	0.001	41.3

[a] Only factors with p-value ≤ α (0.1) were included in the models. In the case of second order effects (i.e. interactions and quadratic terms) the corresponding linear (i.e. first order) terms were also included in the models.[1] [b] The percent contribution of each fitted factor to the prediction formula of the corresponding models was calculated as previously described.

[b] Linear factors with p-values > 0.1 were left in the model if their higher order factors (quadratic or interaction terms) were highly statistically significant.

Derivation of Eq. 1-3 in the main text

Equations 1–3 were derived using multivariate linear regression on the experimentally measured diameters, % yield, and Ψ values, respectively, from 18 experiments (Table 3). These experiments were combinations of the three factors: *t*, *T*, and [*R*]. The procedure used to generate the predictive equations is a standard method in Design of Experiments (DOE) and is outlined as follows (illustrated here using the case of CuNW diameters):

1. Experimental diameter values were collected from the 18 experimental runs.
2. Software (JMP, in our case) performed multivariate regression on the experimental diameter values, resulting in a predictive equation of the form:

   $$\text{diameter} = a \times t + b \times T + c \times [R] + d \times t^2 + e \times T^2 + f \times [R]^2 + g \times t \times T + h \times t \times [R] + i \times T \times [R] + j$$

This is a four-dimensional equation, as it simultaneously analyzes three factors that influence CuNW diameter. The equation contains linear terms (e.g. a × t), quadratic terms (i.e. d × t^2), and interaction terms (e.g. g × t × T).

3. The software also performed a statistical analysis of the factors using analysis of variance (ANOVA), providing p-values for each factor. Factors with p-values greater than 0.1 were considered statistically insignificant (or poorly significant) and were therefore removed from the predictive equation. For example, in the case of CuNW diameters, the factors $t{\cdot}T$, $t{\cdot}[R]$, and t^2 were deemed statistically insignificant and removed from the predictive equation (as they are not included in Equation 1).

Following these procedures, the resulting "simplified" equation describing the diameters is presented as Equation 1 in the main text. The final ANOVA results are provided in Table S1, showing that all factors included in our predictive equations are statistically significant at a p-value ≤ 0.1, with most factors being significant at much lower p-values. This level of statistical significance is generally considered robust, especially in the early stages of research and development.

Table S2. Element percentage resulting from EDX of Fig. S8.

Atom	Percentage (%)
O	1.62
Cu	98.38
Total	100.00

Table S3. Experimental parameters for EDX spectrum acquisition.

Lifetime:	32.0s
Accelerating Voltage:	20.00 kV
Magnification:	49229 x
Working Distance:	8.0 mm
Specimen Tilt (degrees):	0.0
Elevation (degrees):	35.0
Azimuth (degrees):	0.0
Number Of Channels:	2048
Energy Range (keV):	20 keV
Energy per Channel (eV):	10.0 eV
Detector Type Id:	26
Detector Type:	X-Act
Window Type:	SATW

Table S4. Fitting analysis of 3D plot of Fig. 3B.

Equation	$z=z_0+a*x+b*y+c*x^2+d*y^2+f*x*y;$
z_0	1328.43835 ± 410.62007
a	-37.07289 ± 32.30923
b	-18.45594 ± 6.94556
c	-1.95503 ± 4.23161
d	0.06489 ± 0.02755
f	0.42408 ± 0.13885
Reduced Chi-Sqr	420.76778
R-Square (COD)	0.81477
Adj. R-Square	0.68247

Table S5. Fitting analysis of 3D plot of Fig. 3E.

Equation	$z=z_0+a*x+b*y+c*x^2+d*y^2+f*x*y;$
z_0	-116.07614 ± 187.41088
A	14.30378 ± 3.39274
B	0.77106 ± 3.15424
C	-0.25007 ± 0.12446
D	0.00168 ± 0.01259
F	-0.05907 ± 0.01651
Reduced Chi-Sqr	114.98085
R-Square (COD)	0.84348
Adj. R-Square	0.77234

Table S6. Fitting analysis of 3D plot of Fig. 3H.

Equation	$z=z_0+a*x+b*y+c*x^2+d*y^2+f*x*y;$
z_0	-275.2617 ± 71.8907
a	13.05261 ± 3.29254
b	2.90613 ± 1.04674
c	-0.30453 ± 0.06189
d	-0.00779 ± 0.00407
f	-0.03846 ± 0.01509
Reduced Chi-Sqr	12.00277
R-Square (COD)	0.90887
Adj. R-Square	0.85192

Characterization of electrocatalytic tests' products

Both liquid and gaseous products were obtained from the electrocatalytic experiments, which were characterized with Nuclear Magnetic Resonance (NMR) and Gas Chromatography (GC), respectively.
In both cases, the quantitative information (number of produced moles, *n*) about a certain product was acquired by integrating the corresponding peak in the NMR or GC spectrum, then compared with known value.
For liquid products, internal standard concentration was considered and the experimental moles of the specific analyte in the reaction batch were defined as:

$$n_{A,\ experimental} = \frac{C_S \cdot S_A \cdot V_{NMR\ sample}}{S_S \cdot V_{A\ sample}} \cdot V_{tot} \qquad \text{(eq. S1)}$$

Where C_S is the concentration of DMSO standard, S_A is the area of the analyte peak, normalized for the number of protons of the compound, $V_{NMR\ sample}$ is the total volume of the NMR sample (610 μL), S_S is the area of the standard peak, normalized for the number of protons of the compound, $V_{A\ sample}$ is the volume of

analyte solution in the NMR sample (550 μL), and V_{tot} is the volume of the solution in which the reaction occurred (50 mL). Therefore, FE% is calculated as follows in eq. S2

$$FE\ \% = \frac{n_{A,\ experimental}}{n_{A,\ theoretical}} \cdot 100 \qquad \text{(eq. S2)}$$

Where $n_{a,\ theoretical}$ are calculated with eq. S3.
Similarly, the experimental moles of a specific gaseous product ($n_{A,\ experimental}$), were calculated using the percentage volume concentration of the product in the sample injected ($V_{\%}$), with respect to the total volume of gas collected at the end of experiment in the collection bag (V_{bag}) and applying the ideal gas rule:

$$n_{A,\ experimental} = \frac{P \cdot (V_{bag} \cdot V_{\%})}{R \cdot T} \qquad \text{(eq. S3)}$$

P is the atmospheric pressure (1 atm), *T* is the room temperature (23°C) and *R* is the ideal gas constant (0.0821 L atm mol K^{-1}).

3. References

1. C. Y. Lin, S. R. A Marque, K. Matyjaszewski, and M. L Coote, *Macromolecules*, 2011, **44**, 7568-7583.
2. G. Derringer, and R. Suich, *J. Qual. Technol.*, 1980, **12**, 214-219.
3. L. V. Candioti, M. M. De Zan, M. S. Cámara, and H. C. Goicoeche, *Talanta*, 2014, **124**, 123-138.